Condensate partitioning governs the mechanism of action of FUS phase separation modulators

Hannes Ausserwöger[1,*], Daoyuan Qian[1,*], Georg Krainer[1,*], Timothy J. Welsh[1], Tomas Sneideris[1], Titus M. Franzmann[2], Seema Qamar[3], Jonathon Nixon-Abell[3], Mrityunjoy Kar[4], Peter St George-Hyslop[5,6], Anthony A. Hyman[4], Simon Alberti[2], Rohit V. Pappu[7], Tuomas P. J. Knowles[1,8,+]

[1] Centre for Misfolding Diseases, Yusuf Hamied Department of Chemistry, University of Cambridge, Lensfield Road, Cambridge CB2 1EW, United Kingdom

[2] Biotechnology Center (BIOTEC), Center for Molecular and Cellular Bioengineering (CMCB), Technische Universität Dresden, Tatzberg 47/49, Dresden, Germany

[3] Cambridge Institute for Medical Research, Department of Clinical Neurosciences, Clinical School, University of Cambridge, Cambridge, CB2 0XY, United Kingdom

[4] Max Planck Institute of Cell Biology and Genetics (MPI-CBG), 01307 Dresden, Germany

[5] Department of Medicine (Division of Neurology), Temerty Faculty of Medicine, University Health Network, University of Toronto, Toronto, Ontario M5T 0S8, Canada

[6] Department of Neurology, Columbia University, 710 West 168th Street, New York, New York 10032, USA

[7] Department of Biomedical Engineering and Center for Biomolecular Condensates, Washington University in St. Louis, St. Louis, MO, USA

[8] Cavendish Laboratory, Department of Physics, University of Cambridge, JJ Thomson Road, Cambridge CB3 0HE, United Kingdom

* Contributed equally

[+] Correspondence should be addressed to tpjk2@cam.ac.uk

Abstract

Biomolecular phase separation has emerged as a critical process for regulating cellular organisation and function. Modulators, ranging from ionic species to small molecule compounds and macromolecular binders, are key in controlling phase behaviour. The mechanisms of action of such modulators, however, have remained challenging to resolve as means to study protein–modulator interactions within condensates are lacking. Here we unravel biophysical mechanisms of protein phase separation modulation by applying a tie-line-gradient-based analysis approach to characterize the effects of modulators on the partitioning and interactions of species across the dense and dilute phases. Using the protein fused in sarcoma (FUS), we first characterize the impact of ionic species on FUS phase separation and find that potassium chloride (KCl) ions are preferentially excluded from condensates at low ionic strengths as they counteract intermolecular interactions by charge screening. Conversely, in the high salt reentrant phase separation regime, salts preferentially partition into the dense phase thereby scaffolding condensates by enhancing non-ionic interactions. Furthermore, we show that the common phase separation disruptor 1,6-hexanediol decreases FUS phase separation propensity by acting as a solvation agent for the protein. This leads to an expansion of the polypeptide chain, which limits the ability of FUS to form inter- and intramolecular interactions, thereby counteracting condensation. Lastly, we study a sequence-specific modulator of FUS phase separation using a FUS-targeting RNA aptamer and find a concentration-dependent response of condensate stabilisation already at nanomolar concentrations. The sequence-specific binder first partitions as a client molecule into the condensate and then acts as a scaffolder within the condensate. Taken together, our study highlights a broadly applicable approach for studying condensate partitioning allowing us to decipher the mechanisms of action of phase separation modulators.

Introduction

Protein interactions and protein assembly are ubiquitous to life as they enable essential functions such as protein synthesis[1,2], cellular signalling[3,4], and compartmentalization[5,6]. Recently, a new theme for biomolecular function[7], based on protein interactions and protein assembly, has emerged, namely the phase separation of proteins and other molecules into biomolecular condensates[6,8,9]. Through phase separation, proteins demix from a homogenous phase into a protein-rich dense phase and a protein-poor dilute phase[10,11]. This process of protein condensate formation has been shown to be critical in diverse biological processes ranging from gene expression to cellular organization[12–15], and its misregulation has been associated with the emergence of aberrant cellular functions and diverse pathologies[16]. The intrinsically disordered protein fused in sarcoma (FUS), for instance, is a phase separating protein involved in physiologically and pathologically relevant intracellular condensation events[15,17–19] and the emergence of amyotrophic lateral sclerosis (ALS)[15,20,21] and various forms of cancer[22,23].

Importantly, phase separation processes of proteins, including those of FUS, are highly sensitive to modulations[24]. Parameters that control and modulate phase separation include, for example, co-solutes such as ionic salt components[19,25,26], small-molecule compounds[18], as well as sequence-specific binders[27]. Because of their biological significance and sensitivity to modulations, many phase separating protein systems are currently receiving substantial interest as fundamentally novel drug targets to ameliorate human diseases[28,29]. Our understanding of the interactions within condensates and the mechanisms of action of condensate modulators are, however, still limited. For example, it is well established that ionic moieties can act as either the trigger for phase separation or largely prevent it depending on the concentration[25,26]. Despite these drastic effects, questions such as the partitioning of species across the dense and dilute phases or modulation of protein interactions have remain unaddressed. Similarly, aliphatic alcohols are applied regularly to test the dissolution properties and impact of non-ionic interactions on phase separation[30–33]. The biophysical origins of this effect, i.e., how such compounds specifically affect the inter- and intramolecular interactions to alter phase behaviour remains unclear. Lastly, specific sequence-encoded binders such as nucleic acids are well known to have a critical impact on phase separation propensity and influence condensate properties as well as composition[14,18,34]. However, it is difficult to study how these macromolecular binders incorporate into the condensate interaction network as scaffolders to control phase separation.

Common approaches aimed at characterising modulations of phase separation focus on generating phase diagrams that map out conditions under which phase separation occurs[35–37]. Although shifts in phase diagrams and boundaries can provide mechanistic insights, these are typically limited to understanding changes in phase separation propensity as a consequence of the modulator concentration. This, however, does not characterize the protein–modulator interaction and, thus, the mechanism by which the phase separation propensity changes. A critical aspect to characterising a protein–modulator interaction lies in identifying the partitioning of species between the dense and dilute phases. Although this can be studied by fluorescent labelling of species and microscopy analysis of signal colocalization, the readout is majorly influenced by fluorescence quenching and crosstalk between wavelengths[38]. Furthermore, this approach is not applicable to critical phase separation modulators such as ionic species and small molecules, which cannot be fluorescently labelled.

Here, we unravel biophysical mechanisms of protein phase separation modulation by applying a tie-line-gradient-based analysis approach[39] that provides insights into the partitioning and nature of interactions of a protein–modulator condensate system. We highlight the approach by examining phase separation modulation of the protein FUS to dissect how modulators, such as salt species, aliphatic alcohols, and sequence-specific nucleic-acid binders, alter the phase behaviour of FUS. We discover that for phase separation at low ionic strengths, salt ions partition out of the condensates to negate the effect of charge shielding on protein–protein interactions, whereas at high ionic strengths, ions are enriched in the dense

phase to drive non-ionic interactions in the reentrant regime. Furthermore, we show that the commonly used hydrophobic disruptor 1,6-hexanediol modulates FUS phase behaviour by acting as a solvation agent for the protein polypeptide chain. Lastly, we expand our approach to a multicomponent system to contrast these non-specific modulations with a sequence-specific nucleic-acid aptamer binder and show that the highly preferential FUS–aptamer interaction leads to a concentration-dependent condensate stabilisation already in the nanomolar regime. Taken together, our study provides a general blueprint for unravelling mechanisms of phase separation modulation using a tie-line-based approach, thereby shedding light on the biophysical principles underlying condensate formation and modulation.

Results

Tie-line gradients provide insights into the mechanisms of protein phase-separation modulation

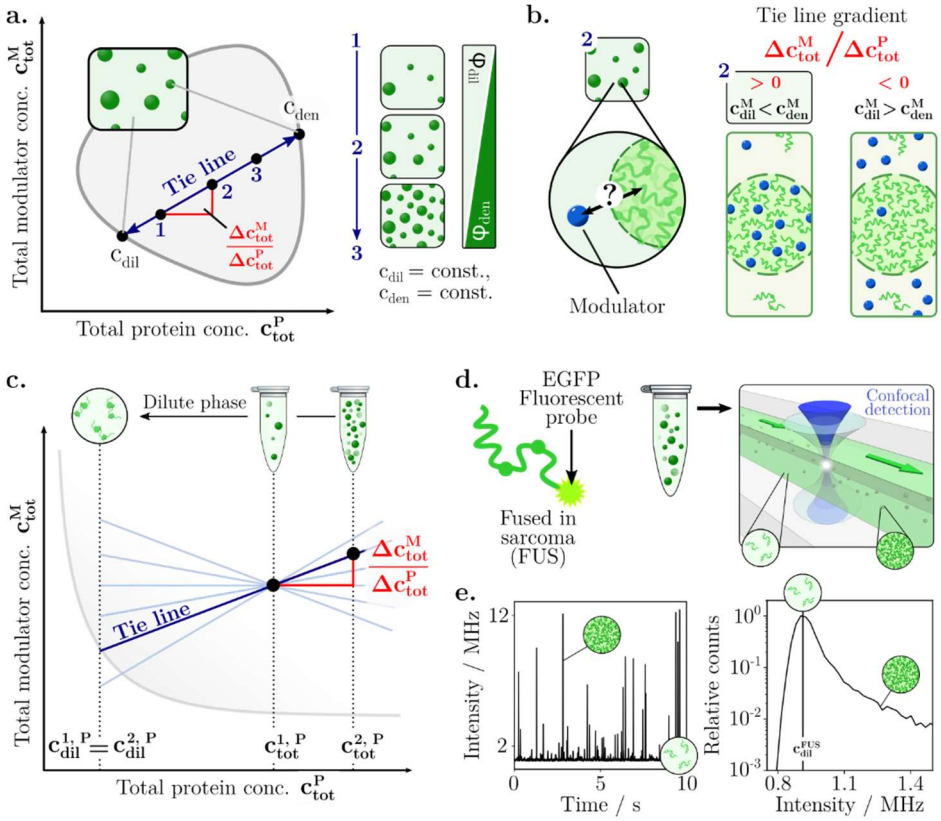

Figure 1. Characterizing protein–modulator tie-line gradients from dilute phase concentration measurements. (a) Schematic of a full phase diagram depicting the concept of tie lines. Tie lines connect the dilute (c_{dil}) and dense phase concentrations (c_{den}) formed via phase separation within the coexistence region of the phase diagram. Total modulator and protein concentrations ($c^{P/M}_{tot}$) within the coexistence region are marked by the grey area. Different combinations of total protein and modulator concentrations (points 1–3), which lie on the same tie line, form the same dilute and dense phase concentrations but display different dilute (ϕ_{dil}) and dense phase volume fractions (ϕ_{den}). **(b)** Tie-line analysis provides insights into the partitioning of species between the dense and dilute phases and enables characterisation of the attractive or repulsive interactions of a protein–modulator condensate system. The tie-line gradient will either be positive or negative, depending on whether the modulator is enriched ($c^M_{den} > c^M_{dil}$) or excluded ($c^M_{den} < c^M_{dil}$) from condensates. **(c)** Concept of determining tie-line gradients ($\Delta c^M_{tot} / \Delta c^P_{tot}$) from measurements of dilute phase protein concentrations (c^P_{dil}) only. Two samples ($X = 1$ and 2) with different total protein ($c^{X,P}_{tot}$) and modulator concentrations ($c^{X,M}_{tot}$), but equivalent dilute phase concentrations will lie on the same tie line. **(d)** Experimental setup to determine dilute phase concentrations of the protein fused in sarcoma (FUS) within a microfluidic channel using confocal detection (see Materials and Methods for details). **(e)** Intensity time trace of a phase separating FUS sample as determined by confocal detection (left panel) and corresponding intensity histogram (right panel). Bursts of high intensity (left panel) correspond to condensates passing the confocal volume. The baseline signal forms a peak in the intensity histogram and is used to calculate dilute phase concentrations. For details, see Materials and Methods.

Our approach to gain mechanistic information on protein phase separation modulation relies on our recently developed tie-line gradient approach[39], adapted here to evaluate protein–modulator condensate systems. A

tie-line connects the dilute and dense phase concentrations formed by a given combination of total protein (c_{tot}^{P}) and modulator concentration (c_{tot}^{M}) within the coexistence region of the phase diagram. Thereby, tie lines serve to describe the partitioning of individual species between the dense and the dilute phases (Fig. 1a)[39]. Hence, if a protein–modulator system displays a positive tie-line gradient ($K = \Delta c_{dil}^{M} / \Delta c_{dil}^{P} > 0$), both species are present at higher concentrations in the dense phase than in the dilute phase. By contrast, a negative tie-line gradient ($K = \Delta c_{dil}^{M} / \Delta c_{dil}^{P} < 0$) suggests that while the protein is enriched in the dense phase, the modulator shows a higher concentration in the dilute phase than in the dense phase, indicating that the modulator is excluded from condensates (Fig. 1b).

To extract tie-line gradients K, it is sufficient to measure dilute phase protein concentrations only (Fig. 1c). This is because points on the same tie line demix into the same c_{dil} and c_{den}, only differing in the volume fractions (ϕ) of the dense and dilute phases formed (Fig. 1a). Experimentally, we obtain tie-line gradients from measurements of dilute phase concentrations by injecting phase separated samples into a microfluidic device and reading out their fluorescence signal by confocal detection. The workflow is exemplified in Figure 1d for the protein FUS, used throughout this study. The drastic increase in sampling achieved by the application of microfluidics allows to extract the dilute phase concentrations from the baseline signal in the fluorescence time traces. The presence of the dense condensate phase is detected from short bursts of high photon intensities stemming from the high protein concentrations within condensates (Fig. 1e). By repeating these dilute phase concentration measurements for different combinations of total protein and modulator concentrations, phase-separated conditions with similar dilute phase concentrations can be identified (Fig. 1b). Through interpolation between points, this procedure allows determining points, which display the same dilute phase concentrations to then calculate the tie-line gradients of the protein–modulator system under scrutiny. In the following, we apply this strategy to mechanistically dissect how common modulators such as salt ions, small molecules, or a nucleic acid aptamer act on condensates to alter the phase behaviour of FUS.

Potassium chloride is excluded from the condensed phase at low concentrations to strengthen protein–protein interactions

Electrostatic interactions are one of the key driving forces for protein condensation and govern important properties of condensates such as colloidal stability and propensity to fuse[19,40]. As such, changes in ionic strength and hence the screening of charged interactions typically has a substantial impact on phase separation behaviour[19,41,42]. Moreover, the cellular environment is characterized by the presence of a complex distribution of cationic and anionic chemical moieties, and as such understanding the differential impact of salt species on phase separation is key. To examine such effects on a mechanistic level, we set out to characterize the partitioning and interactions of FUS in the presence of potassium chloride (KCl) (see Fig. 2a) by performing tie-line gradient analysis.

We first examined the phase separation behaviour of FUS with respect to low concentrations of KCl. To this end, we measured the dilute phase concentrations of FUS (c_{dil}^{FUS}) at 1 and 2 µM total protein concentration (c_{tot}^{FUS}) and KCl concentrations (c_{tot}^{KCl}) ranging from 20 to 150 mM (Fig. 2b). c_{dil}^{FUS} was determined to be constant at high KCl concentrations ($c_{tot}^{KCl} > 100$ mM) as the protein did not undergo phase separation in this regime (see Fig. 2b). At lower KCl concentrations ($c_{tot}^{KCl} \sim 40$–75 mM, depending on protein concentration), a drop-off in c_{dil}^{FUS} and the appearance of high-intensity bursts were observed, corresponding to the onset of phase separation. At even lower KCl concentrations, the dilute phase concentration of FUS dropped further. As such, a higher phase separation propensity was observed at lower salt concentrations, in agreement with previous observations[19,25]. This indicates that KCl screens intermolecular interactions at higher concentrations (Fig. 2b), while at lower KCl concentrations more pronounced protein interactions occur, leading to the formation of condensates. This behaviour is also represented by the phase boundary of the system (Fig. 2c), which can be predicted from the changes in dilute phase concentrations and the tie-line gradient (see Material and Methods)[39]. This shows that phase separation only occurs below a certain KCl

concentration threshold, and for phase separation to become favourable at higher salt concentrations, higher protein concentrations are necessary.

We then used the dilute phase concentrations measurements (shown in Fig. 2b) to determine the tie-line gradient between FUS and KCl. Considering the dissociation of the salt into ionic species, the measured tie-line gradients correspond to the ratio of protein to a weighted average of the cationic and anionic species, with the weights relating to their valency (see Supplementary Information). In doing so, a negative gradient of $\Delta c_{tot}^{KCl} / \Delta c_{tot}^{FUS} = -19 \pm 10$ mM/µM was obtained. This indicates that the overall KCl concentration is lower in the dense phase as compared to the dilute phase. Although the partitioning pattern of both Cl^- and K^+ is not assessed individually, on average, the ions are preferentially excluded from the condensate to allow for a decrease in the electrostatic screening and more pronounced protein–protein interactions in the dense phase to occur, in agreement with previous simulation results for FUS condensates[40]. A similar behaviour has also been observed before for polyelectrolyte polymers where the preferential exclusion of ions from the condensed phase acts as a driving force for assembly[43,44], hence, supporting the proposed interaction mechanism for FUS.

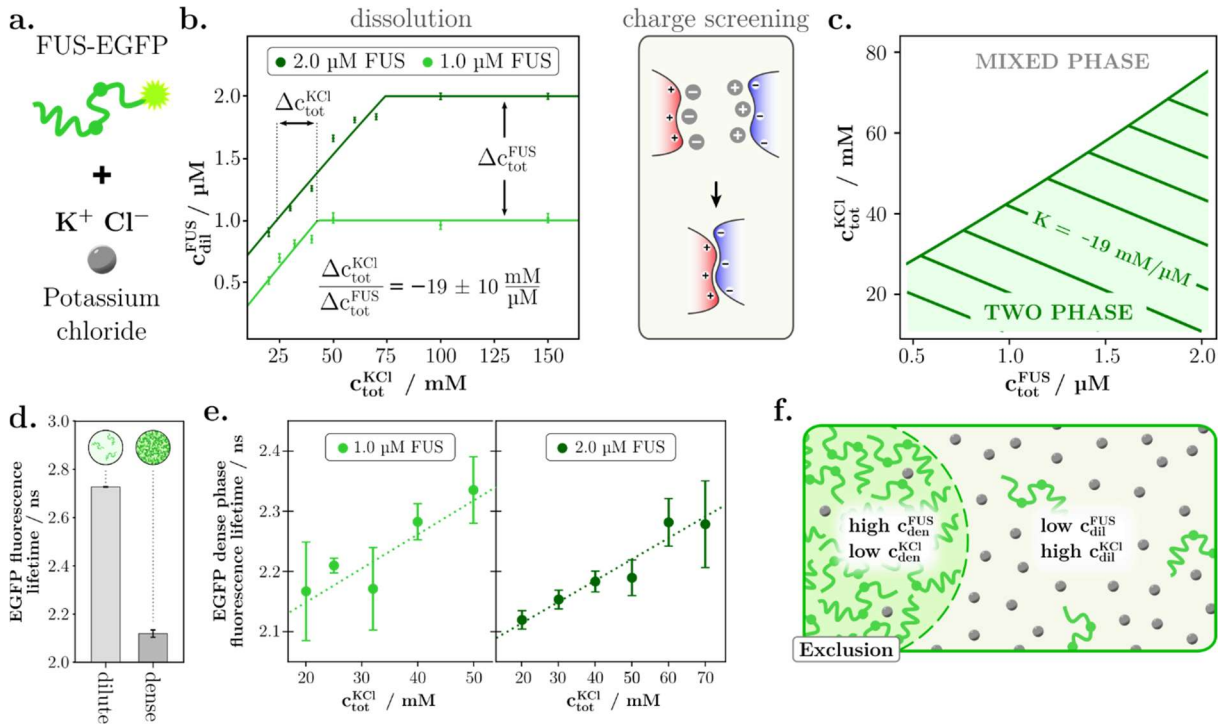

Figure 2. Potassium chloride is preferentially excluded from FUS condensates. (a) Phase separation of FUS-EGFP was studied in the presence of potassium chloride (KCl). **(b)** Dilute phase concentration changes of FUS (c_{dil}^{FUS}) at varying total KCl concentrations (c_{tot}^{KCl}). A negative tie-line gradient ($\Delta c_{dil}^{KCl} / \Delta c_{dil}^{FUS}$), indicative of charge screening, was determined. Experiments were performed at 1 µM (light green) and 2 µM (dark green) total FUS concentration (c_{tot}^{FUS}). **(c)** Extrapolated phase boundary highlights that phase separation occurs only below critical KCl concentrations. **(d)** Comparison of EGFP fluorescent lifetime signal in the dense and dilute phase at 2 µM FUS and 20 mM KCl. **(e)** Condensate fluorescent lifetimes of the EGFP-tag on the FUS protein decreases with the reduction of KCl. **(f)** Schematic illustration summarizing the partitioning behaviour of KCl between the dense (c_{den}^{KCl}) and the dilute phases of FUS.

The preferential exclusion of KCl from the dense condensate phase suggests that the condensate scaffold and environment might change drastically with salt concentration. To investigate this further, we determined the fluorescence lifetime of the EGFP protein tag on FUS as a function of varying KCl concentrations. Distinctly different lifetimes were observed for the dilute phase and the condensate phase ($\tau_{dil} \sim 2.727$ vs $\tau_{den} < 2.35$ ns, changing with KCl concentration, see Fig 2d). The much shorter lifetime of the dense phase indicates a higher refractive index due to the locally higher protein concentration within the condensates[45,46]. Crucially, the fluorescence lifetime of the condensed phase was determined to decrease further with decreasing KCl

concentration ($\tau_{\text{cond, 70 mM KCl}}$ = 2.28 ± 0.07 ns, $\tau_{\text{cond, 20 mM KCl}}$ = 2.12 ± 0.02 ns, both at 2 µM FUS) (see Fig. 2e). Hence, FUS condensates become more densely packed, indicative of enhanced protein interactions through the removal of potassium chloride ions. This further supports our observations above that exclusion of ions from the dense phase acts as the key trigger for phase separation through a reduction of charge shielding, thereby allowing for more favourable FUS–FUS contacts to occur (see Fig. 2f).

Ions partition into FUS condensates at high salt concentrations to drive non-ionic interactions

FUS, as well as other proteins, have been shown to display phase separation at high salt concentrations within a so-called reentrant phase separation regime[25] (Fig. 3a). Here, changes in the elemental anion and cation species in particular have been shown to yield large shifts in the saturation concentrations required to induce the phase separation. To further investigate the mechanism by which ions can trigger phase separation in the high concentration reentrant regime, we performed tie-line gradient analysis of FUS in the presence of high concentrations of lithium chloride (LiCl) and caesium chloride (CsCl). Both LiCl and CsCl have been previously shown to display large differences in the saturation concentration[25], however, the mechanistic basis of this behaviours has remined elusive.

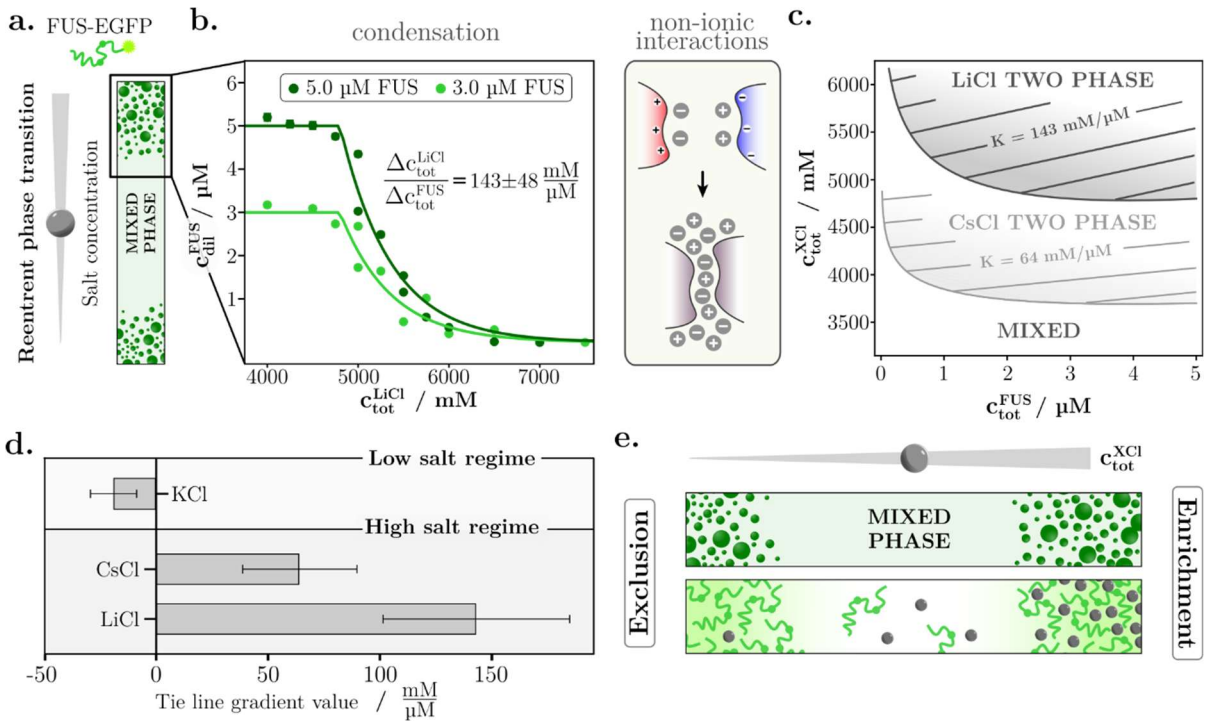

Figure 3. Salt ions are enriched in high salt reentrant FUS condensates to foster non-ionic interactions. (a) FUS displays reentrant phase separation at high salt concentrations. **(b)** Dilute phase concentration changes of FUS (c_{dil}^{FUS}) at varying total LiCl concentrations (c_{tot}^{LiCl}), from which a positive tie-line gradient (Δc_{dil}^{LiCl} / Δc_{dil}^{FUS}) is determined. This preferential partitioning of ions into the condensate phase indicates that the salt species shield ionic and polar interactions to drive phase separation through non-ionic interactions. Experiments were performed at 3 µM (light green) and 5 µM (dark green) total FUS concentration (c_{tot}^{FUS}). Experiments were performed in a similar manner for CsCl (see Supplementary Figure 5). **(c)** Extrapolated phase boundaries show that phase separation occurs only above the respective critical salt concentrations. **(d)** Comparison of tie-line gradients between in the low salt and high salt reentrant regime. **(e)** Schematic illustration summarizing the mechanism of phase separation in the low and high salt regime. At low salt conditions, phase separation is caused by exclusion of ions from the dense phase to allow for enhanced electrostatic protein–protein interactions as indicated by a negative tie-line gradient. Conversely at high salt conditions, ions preferentially partition into condensates to drive non-ionic interactions as shown by a positive tie-line gradient.

We first characterised the change in dilute phase concentration of FUS-EGFP under varying concentrations of LiCl at 3 and 5 µM total protein concentration (c_{tot}^{FUS}) and LiCl concentrations varying between 4 and 7.5 M (Fig. 3b). Indeed, a rapid drop-off in c_{dil}^{FUS}, indicated by the onset of reentrant phase separation, was

observed at around 5 M LiCl, consistent with previous observations[25]. The critical concentrations were very similar for both protein concentrations, hence, indicating that the changes in protein concentration have a small effect on the saturation concentration, which is largely determined by the type of salt (Fig. 3c). In addition, c_{dil}^{FUS} decreased to almost 0 µM protein concentration at high LiCl concentrations, suggesting that in this 'salting out' regime, the protein is almost completely sequestered into the condensed phase.

From the changes in c_{dil}^{FUS} with varying LiCl concentrations, we then determined the tie-line gradient between FUS and LiCl to be $\Delta c_{tot}^{LiCl} / \Delta c_{tot}^{FUS} = 143 \pm 48$ mM/µM. Therefore, LiCl at high salt concentrations, due to the positive tie-line gradient, displays preferential partitioning into condensates and an attractive interaction between the ions and the protein. This is supported by the commonly proposed mechanism for reentrant phase separation, which suggest that the drastic increase in ionic strength brings forth strong non-ionic interactions between the protein molecules. Accordingly, recruitment of ions into the condensed phase will strengthen these non-ionic interactions through shielding of ionic and polar interactions. Hence, in the high salt reentrant regime, the salt displays an opposing dense phase partitioning trend compared to the low ionic strength regime (Fig 3d, e), where the ions counteract protein–protein interactions, which drive ion exclusion from the condensed phase.

Next, we characterised changes in c_{dil}^{FUS} as a function of CsCl concentrations (Supplementary Fig. 1) to elucidate the impact of changes in the cation. Phase separation was already observed at approx. 3.8 M CsCl compared to a saturation concentration of around 5 M for LiCl, in accordance with previous observations[25], indicating that CsCl is more potent at triggering reentrant phase separation of FUS. This is also highlighted by the dilute phase concentration changes, where a much steeper drop-off in c_{dil}^{FUS} is observed when increasing CsCl (see Fig. 3b and Supplementary Fig. 1). This is further reflected in the tie-line gradient for CsCl with FUS, which was determined as $\Delta c_{tot}^{LiCl} / \Delta c_{tot}^{FUS} = 64 \pm 25$ mM/µM compared to $\Delta c_{tot}^{LiCl} / \Delta c_{tot}^{FUS} = 143 \pm 48$ mM/µM for LiCl. This indicates that CsCl partitions less strongly into the condensed phase, suggesting that less ions are required to allow for sufficient non-ionic interactions occur to trigger phase separation. This is further highlighted by the fact that the tie-line gradient appear to be closely linked to the solubility of the salts individually with c_{sat}^{LiCl} being 13.4 M ($K = 143$ mM/µM) and c_{sat}^{CsCl} being 5.9 M ($K = 64$ mM/µM) (according to supplier specification) as well as following the expected trend of the Hofmeister series[47].

Taken together, our findings highlight that salt species in the high salt reentrant regime preferentially partition into condensates, and that the degree of partitioning is closely related to the propensity of the individual salts to trigger phase separation.

1,6-hexanediol alters the solvation properties of FUS to destabilize the condensed phase

Hydrophobic and non-ionic interactions are not only critical to driving phase separation in the high salt reentrant regime but have been highlighted as a key driver of phase separation also at or below physiological salt concentrations. These hydrophobic interactions can be modulated by aliphatic alcohols, such as 1,6-hexanediol (1,6-HD), often causing dissolution of condensates[25,48]. Applying compounds like 1,6-HD has become a powerful strategy for studying phase separation to investigate the nature of interactions underlying the condensate formation or assess the liquidity of condensates[30–33]. It is, however, largely unclear how the protein physico-chemical properties and intermolecular interactions are specifically altered in the presence of 1,6-HD to achieve these modulations.

To shed light on the mechanism of action of 1,6-HD through tie-line analysis, we first measured changes in c_{dil}^{FUS} in the absence and presence of 1,6-HD. To do so, at a total FUS concentration of 1 and 2 µM, the total PEG concentration was varied from 0–8 % (w/v) to induce phase separation of FUS (Fig. 4a). In the absence of 1,6-HD, phase separation of FUS was observed already at a PEG concentration of 2–3 % (w/v), leading to a decrease in c_{dil}^{FUS}. As expected, the addition of 1,6-HD led to a reduced propensity of FUS to undergo phase separation, as much higher PEG concentrations were necessary to induce phase separation.

Accordingly, a decrease of c_{dil}^{FUS} was observed only at around 5–6 % (w/v) PEG. This is also reflected in the shift of the phase boundary, which shows that higher concentrations of PEG are necessary to induce phase separation of FUS in the presence of 1,6-HD (Fig. 4b). These results are in agreement with the dissolution properties commonly associated with 1,6-HD[25,30,49].

We further determined the FUS/PEG tie-line gradient (Fig. 4c), both in the presence and absence of 1,6-HD. The shift in the tie-line gradient then describes changes in the FUS-PEG interaction based on the introduction of 1,6-HD. Interestingly, the tie-line gradient decreased from $\Delta c_{tot}^{PEG} / \Delta c_{tot}^{FUS} = 0.69 \pm 0.15$ % (w/v) / µM without hexanediol to $\Delta c_{tot}^{PEG} / \Delta c_{tot}^{FUS} = 0.38 \pm 0.12$ % (w/v) / µM in presence of 1,6-HD. Crucially, the tie-line gradient is proportional to the dense-phase molar stoichiometry ratio of constituent components[39]. Therefore, these results suggest that the presence of 1,6-HD decreases the amount of PEG copolymers per FUS molecule by approximately half within condensates. Such a decrease in copolymer partitioning points toward a decrease in the self- or cross-interaction propensity of FUS, which could be explained by 1,6-HD functioning as a solvation agent of the protein.

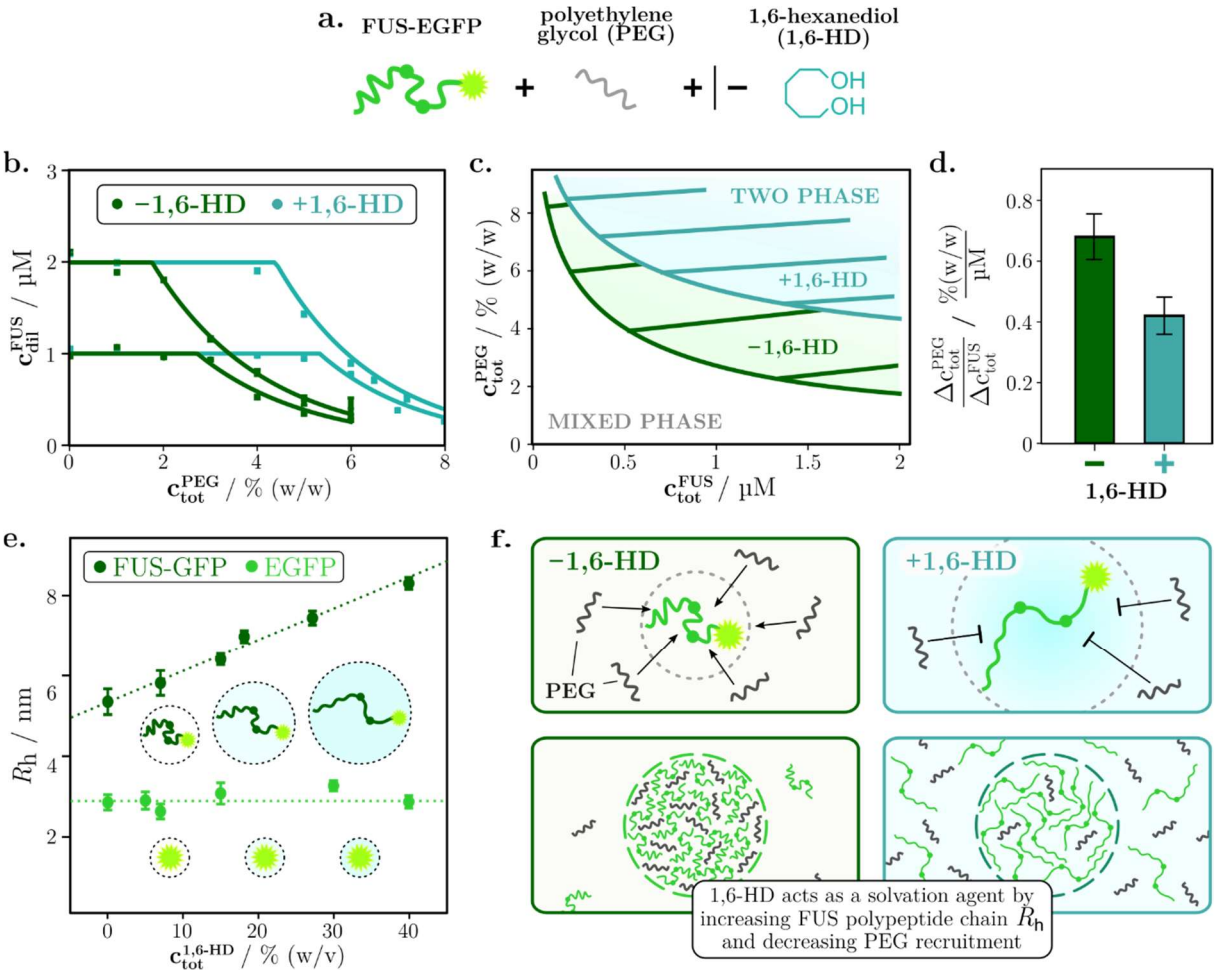

Figure 4. 1,6-hexanediol (1,6-HD) decreases the phase separation propensity of FUS by acting as a solvation agent. **(a)** To characterise the mechanism of action of 1,6-hexanediol phase separation of FUS with PEG was studied in presence (+) and absence (-) of the compound. **(c)** Dilute phase FUS concentration changes with varying concentrations of PEG at 1 and 2 µM FUS protein concentration in the presence (+) and absence (-) of 1,6-HD (7% (w/v)). **(c)** Predicted phase boundaries for FUS in the absence and presence of 1,6-HD created from changes in dilute phase concentrations and tie-line gradients. **(d)** Shift in tie-line gradient of FUS/PEG in the absence and presence of 1,6-HD. **(e)** Changes in hydrodynamic radius R_h as a function of 1,6-HD concentration. Shown are data for monomeric FUS-EGFP (dark green) and EGFP protein alone (light green) at 1 µM protein concentration each. **(f)** Schematic illustration depicting the improved solvation of FUS in the presence of 1,6-HD, which leads to a reduction of the protein's propensity for intra- and intermolecular interactions, as indicated by the expansion of the polypeptide chain and a decrease in PEG molecules that are recruited into FUS condensates.

Such improved solvation of an intrinsically disordered protein would be expected to lead to an expansion of its polypeptide chain. To test this hypothesis and to rationalise the mechanism of action of 1,6-HD, we set out to characterise the impact of the compound on the structure of the monomeric protein. Using microfluidic diffusional sizing[50], we determined the hydrodynamic radius (R_h) of monomeric FUS-EGFP at different concentrations of 1,6-HD. Strikingly, we indeed identified a significant increase of the protein's hydrodynamic radius with increasing 1,6-HD concentrations (Fig. 4d). As a control, the R_h of EGFP alone was monitored at the same 1,6-HD concentrations where no increase in R_h was observed. This expansion in protein size indeed suggests that 1,6-HD acts as a solvation agent for the FUS polypeptide chain, and likely in particular of the intrinsically disordered regions of FUS (Fig. 4e). Thereby, the intramolecular interactions between amino-acid residues causative for protein compaction are disrupted by 1,6-HD and, hence, become less favourable in presence of 1,6-HD, causing the 1,6-HD co-solvated protein to expand in size. Not only are these self-interactions critical to the condensation process of the protein, as interactions with other FUS molecules drives phase separation, but similarly the PEG–FUS cross-interaction will become much less favourable.

Taken together, our data show that 1,6-HD disrupts phase separation by improving the solvation of the FUS polypeptide chain, which at the same time limits its ability to interact with and recruit further copolymers in the condensed phase.

A concentration dependent client-to-scaffolder transition of a FUS targeting aptamer

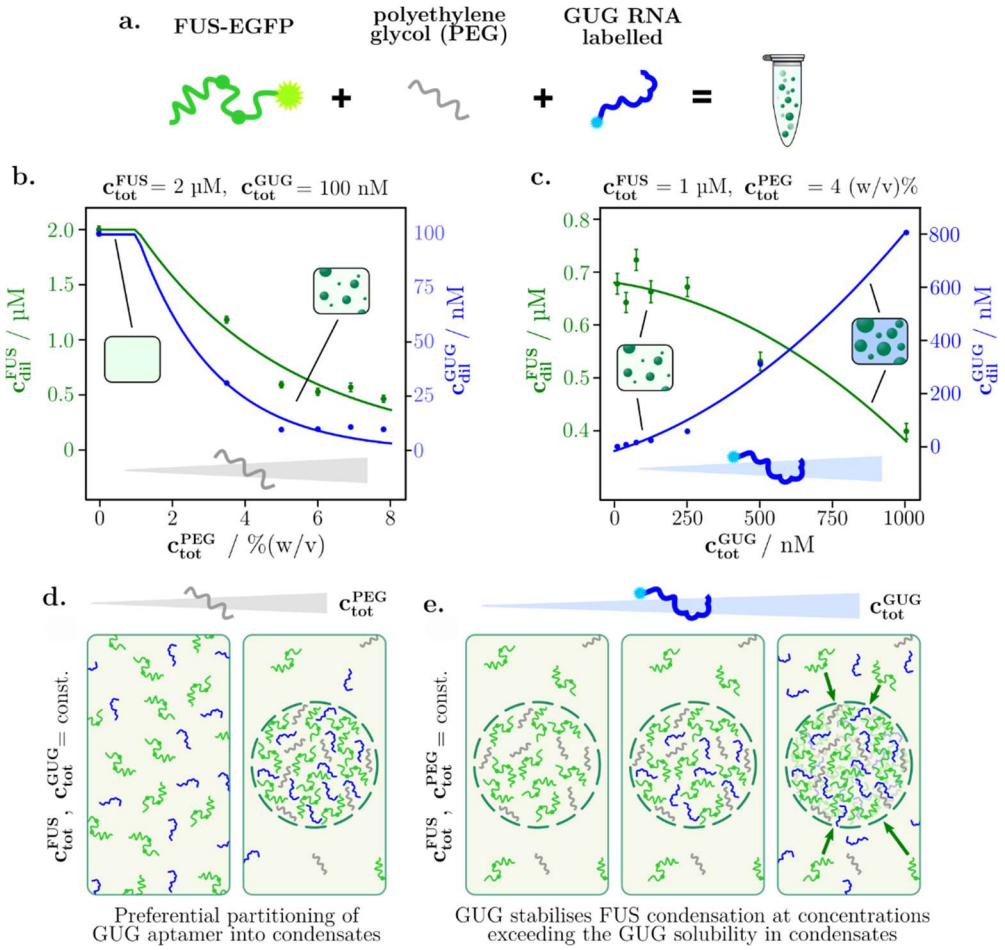

Figure 5. GUG aptamers partition into and stabilize FUS–PEG condensates. (a) Condensate system involving FUS, PEG and the FUS targeting GUG aptamer. Dilute phase concentration changes in FUS (green) and GUG aptamer (blue) are traced simultaneously while **(b)** varying PEG and **(c)** varying GUG aptamer concentrations. The total concentrations of the other two components are kept constant. **(d, e)** Schematic illustration of the system's response to changes in PEG (panel d) and GUG aptamer (panel e) concentration. An increase in PEG concentration causes phase separation of FUS and preferential partitioning of GUG

aptamer into condensates (panel d). At increasing concentrations of GUG aptamer, FUS condensates are stabilised after the GUG aptamer solubility within condensates is approached (panel e).

Condensates in vivo are characterised by the high multidimensionality of components capable of modulating and interacting with them. As such, in addition to salts or small-molecule compounds, phase separation is majorly affected by specific macromolecular binders like nucleic acids. FUS, for example, is an RNA-binding protein harbouring a specific subdomain for interactions with nucleic acids[51,52]. As such, specific nucleic-acid binders are expected to engage in interactions with the protein at much lower concentrations and thereby modulate phase behaviour by altering the interaction network within condensates. To probe such specific phase separation modulation events in a higher dimensional system through tie-line analysis, we study the impact of the 'GUG' aptamer (see Supplementary Information for sequence), which has previously been reported to interact with FUS[18,27,53] and FUS condensates[53] (Fig. 5a) on FUS phase separation in presence of PEG as an additional scaffolding polymer.

First, we characterised the dilute phase concentrations of the FUS/GUG aptamer system in response to changes in the concentrations of PEG as the phase separation trigger. This was done at a constant, total FUS concentration $c_{tot}^{FUS} = 2$ µM and a total GUG aptamer concentration of $c_{tot}^{GUG} = 100$ nM, while c_{tot}^{PEG} was varied from 0–8% (w/v) (Fig. 5b). Phase separation was observed at PEG concentrations > 3% (w/v), evident by a decrease in dilute phase FUS concentration. Similar to FUS, the GUG aptamer dilute phase concentration c_{dil}^{GUG} decreased with increasing PEG concentrations. This indicates that the GUG aptamer partitions into the dense condensate phase. At 8% (w/v) PEG, for example, the dilute phase concentration of GUG aptamer dropped to $c_{dil}^{GUG} \sim 10$ nM compared to a total concentration of $c_{tot}^{GUG} = 100$ nM. This equates to a dilute phase fraction $c_{dil}^{GUG}/c_{tot}^{GUG}$ of ~ 0.1 as a result of GUG aptamer partitioning into condensates. This represents an even higher enrichment of GUG aptamer in condensates than of FUS protein itself, for which a dilute phase fraction $c_{dil}^{FUS}/c_{tot}^{FUS}$ of ~ 0.3 was determined at 8% (w/v) PEG).

We next set out to characterise the system's response to varying concentrations of GUG aptamer by keeping FUS and PEG concentrations constant at $c_{tot}^{FUS} = 1$ µM and $c_{tot}^{PEG} = 4\%$ (w/v), and varying the GUG aptamer concentration between $c_{tot}^{GUG} = 0$–1000 nM (Fig. 5c). In this regime, condensates readily formed, allowing us to examine the stabilization via changes in dilute phase concentration. In line with the results from the PEG variation experiment above, c_{dil}^{GUG} only increased marginally at lower concentrations of GUG aptamer (< 250 nM), as evident by a dilute phase fraction of $c_{dil}^{GUG}/c_{tot}^{GUG} \sim 0.2$ throughout the concentration range tested. This indicates that the majority of GUG aptamer molecules are sequestered into condensates. Interestingly, c_{dil}^{FUS} remained roughly constant in this regime, suggesting that the FUS condensate stability is largely unaffected by the aptamer partitioning. However, when increasing c_{tot}^{GUG}, c_{dil}^{GUG} started to increase drastically, also evident by an increase in $c_{dil}^{GUG}/c_{tot}^{GUG} > 0.5$. This indicates that the saturation capacity of the GUG aptamer within the condensate is being approached. This increase in c_{dil}^{GUG} coincides with a decrease in c_{dil}^{FUS} (Fig. 5c). Hence, at concentrations above the solubility of the GUG aptamer within FUS condensates, the GUG aptamer starts to stabilize the condensed phase by recruiting more FUS into condensates (Fig. 5d, e). This is likely due to a highly preferential FUS–GUG aptamer interaction, arising from the formation of sequence specific binding events and weaker multivalent backbone interactions within condensates compared to the pairwise/dimeric dilute phase interaction.

To confirm the preferential interaction of GUG aptamer within condensates, we set out to characterise the three-dimensional (3D) tie-line gradient between FUS, GUG aptamer and PEG. Similar to the two-dimensional tie-line analysis performed above, we screened for conditions of equivalent dilute phase concentration pairs of both FUS and GUG aptamer. By projecting both concentration variation experiments onto the dilute phase FUS vs. dilute phase GUG plane, the intersection point can be extrapolated by fitting to the dilute phase data (see Supplementary Fig. S1). In doing so, the 3D tie-line gradient can be determined with $\Delta c_{tot}^{FUS} / \Delta c_{tot}^{GUG} / \Delta c_{tot}^{PEG}$ = +1 µM / +18 nM / +1.4% (w/v). Crucially, all three species display a

positive tie-line gradient. This corroborates the observations from the observed dilute phase concentration changes above, that all three components partition into the condensates and display preferential attractive interactions between them in the dense phase.

Discussion

In this work, we have dissected the biophysical mechanisms of FUS phase separation modulators using a tie-line-based approach that relies on measuring dilute phase concentrations only (Fig. 1). Specially, we have explored the impact of ionic species on phase separation. We have shown that at low salt concentrations, KCl ions are preferentially excluded from condensates, which strengthens intermolecular interactions within the dense phase (Fig. 2). At high salt concentrations, an opposing trend is observed, where LiCl and CsCl ions preferentially partition into condensates to drive non-ionic interactions in the reentrant regime (Fig. 3). Furthermore, we have shown that 1,6-HD disrupts condensates by acting as a solvation agent for FUS, as determined by an expansion of the polypeptide chain with increasing 1,6-HD concentrations, which also limits the ability of FUS to recruit PEG co-polymers (Fig. 4). Lastly, we contrast these non-specific modulators by characterising the impact of the FUS targeting GUG RNA-aptamer, which shows a concentration dependent stabilisation effect on FUS condensates in the nanomolar concentration range (Fig. 5).

The exclusion of ions at lowered KCl concentrations bear potential wide-ranging implications for cell physiology and disease. The conductance of chloride ions is a pivotal feature in neuronal transmission and plays an important role in controlling cell excitability. Depending on the neuronal subtype and excitation state, intracellular chloride ion levels can vary from a few millimolar to above a hundred millimolar[54]. Additionally, intracellular chloride levels can be dramatically altered by changes in the expression levels of various ion channels, in the context of pathology[55,56]. Given the profound impact of KCl on FUS phase separation, we speculate that changes in intracellular chloride ion concentrations could serve to modulate phase separation of FUS and possibly other proteins in cells, hence, being a potentially indicative of a dynamic control mechanism of phase separation propensity and condensate composition in cells.

Our investigations into metal halide salt partitioning between the dense and dilute phase of FUS condensates at both high and low salt regimes highlight that even relatively simple molecules like salts can display opposing partitioning behaviour. Specifically, in the low salt regime, KCl largely preventative of phase separation as they apprehend protein interactions by charge screening. Therefore, phase separation occurs upon decreasing the salt concentration and, hence, it becomes favourable to exclude the ions from the dense phase. Conversely in the high salt regime, the increase of LiCl and CsCl salt concentration act as the trigger for phase separation by allowing for non-ionic interactions to occur, hence, favouring ion enrichment in the condensed phase. More generally, this might indicate that the partitioning of molecular phase separation modulators is largely a consequence of their propensity to enhance or counteract phase separation.

1,6-HD is one of the most commonly used phase separation modulators in the study of condensate stability, dissolution effects, and numerous other aspects[25,30–33]. Its mechanism of action is broadly agreed upon as a disruption of hydrophobic interactions[25]. Here, we reveal more detailed mechanistic information with respect to its effect on phase separation by highlighting how 1,6-HD acts as a solvating agent for FUS. Given the common presence of intrinsically disordered regions in phase separating proteins, this mechanism of action might translate to other proteins, where 1,6-HD similarly acts as a disruptor. Furthermore, our mechanistic study of 1,6-HD suggests that affecting the FUS protein native state and its chain expansion is a powerful avenue for modulating phase behaviour. Hence, screening for molecules capable of inducing expansion or compaction of intrinsically disordered proteins might be a simple but effective drug discovery strategy. Taken together, our study shows that the tie-line-based biophysical characterisation of 1,6-HD modulation allows for illuminating novel insights to the mechanism of action of even such a common and well understood modulator.

Our data suggests that non-specific modulators like salts or 1,6-HD act by altering the repulsive and solvation properties of the protein in the native state. By comparison, the specific modulation from the GUG aptamer is driven by sequence-encoded interactions with the protein. Accordingly, these interactions become favourable already at much lower concentrations (i.e., at nanomolar concentration as compared to millimolar concentrations for KCl). The sequence-encoded interactions further appear to foster the ability of specific binders to act preferentially on the condensed phase, as GUG aptamer is strongly sequestered into condensates. Preferential partitioning into condensates seems to be driven by the availability of large numbers of interaction sites and eventually integration into the condensate interaction network. Further addition of GUG results in an increased stabilisation of the condensate phase, thus underscoring that RNA can behave first as a client and then as a scaffold within condensates. Overall, the complexity and multifaceted nature of protein–RNA interactions inside and outside of condensates highlights the enormous value of being able to characterise condensate partitioning and interactions across multiple species.

Taken together, by measuring changes in the dilute phase concentration we dissect heterogeneous interactions between multiple species within condensates to generate a fundamental novel biophysical understanding of protein phase separation modulation. In the study of the GUG aptamer specifically, the dilute phase concentrations of FUS and the GUG aptamer allowed us to characterise concentration dependent partitioning in a multidimensional fashion. Changes in the dilute phase concentration can then be further used to determine tie-line gradients, which allow for the study of modulator species, such as salt ions or small molecule compounds, which would otherwise be inaccessible by conventional labelling or detection strategies. Lastly, the effect of modulators on a given protein-scaffolder interaction system can be assessed by characterising the change of the protein-scaffolder tie-line gradient in presence and absence of the modulator, as shown for the FUS-PEG system under the influence of 1,6-HD. Hence, the tie-line gradient analysis approach promises to be a powerful tool for elucidating mechanisms of phase separation modulation in a wide range of contexts such as dissecting the impact of potential novel drug candidates and utilizing mechanistic insight to rationally design more efficacious therapeutics; studying the impact of biologically relevant molecular species on *in vivo* phase transitions; and optimising designer phase separation systems for functional applications.

References

1. Gallie, D. R. Protein-protein interactions required during translation. *Plant Molecular Biology* **50**, 949–970 (2002).
2. Guarracino, D. A., Bullock, B. N. & Arora, P. S. Mini review: protein-protein interactions in transcription: a fertile ground for helix mimetics. *Biopolymers* **95**, 1–7 (2011).
3. Pawson, T. & Nash, P. Assembly of cell regulatory systems through protein interaction domains. *Science* **300**, 445–452 (2003).
4. Pawson, T. & Nash, P. Protein-protein interactions define specificity in signal transduction. *Genes Dev* **14**, 1027–1047 (2000).
5. Chen, A. H. & Silver, P. A. Designing biological compartmentalization. *Trends in Cell Biology* **22**, 662–670 (2012).
6. Hyman, A. A., Weber, C. A. & Jülicher, F. Liquid-liquid phase separation in biology. *Annual review of cell and developmental biology* **30**, 39–58 (2014).
7. Boeynaems, S. *et al.* Protein Phase Separation: A New Phase in Cell Biology. *Trends in Cell Biology* **28**, 420–435 (2018).
8. Banani, S. F., Lee, H. O., Hyman, A. A. & Rosen, M. K. Biomolecular condensates: organizers of cellular biochemistry. *Nature Reviews Molecular Cell Biology* **18**, 285–298 (2017).
9. Shin, Y. & Brangwynne, C. P. Liquid phase condensation in cell physiology and disease. *Science* **357**, eaaf4382 (2017).
10. Brangwynne, C. P., Tompa, P. & Pappu, R. V. Polymer physics of intracellular phase transitions. *Nature Physics* **11**, 899–904 (2015).
11. Alberti, S., Gladfelter, A. & Mittag, T. Considerations and Challenges in Studying Liquid-Liquid Phase Separation and Biomolecular Condensates. *Cell* **176**, 419–434 (2019).
12. Kedersha, N. & Anderson, P. Mammalian Stress Granules and Processing Bodies. in *Methods in Enzymology* vol. 431 61–81 (Academic Press, 2007).
13. Wolozin, B. & Ivanov, P. Stress granules and neurodegeneration. *Nature Reviews Neuroscience* **20**, 649–666 (2019).

14. Guillén-Boixet, J. *et al.* RNA-Induced Conformational Switching and Clustering of G3BP Drive Stress Granule Assembly by Condensation. *Cell* **181**, 346-361.e17 (2020).
15. Patel, A. *et al.* A Liquid-to-Solid Phase Transition of the ALS Protein FUS Accelerated by Disease Mutation. *Cell* **162**, 1066–1077 (2015).
16. Alberti, S. & Dormann, D. Liquid-Liquid Phase Separation in Disease. *Annu Rev Genet* **53**, 171–194 (2019).
17. Murakami, T. *et al.* ALS/FTD Mutation-Induced Phase Transition of FUS Liquid Droplets and Reversible Hydrogels into Irreversible Hydrogels Impairs RNP Granule Function. *Neuron* **88**, 678–690 (2015).
18. Maharana, S. *et al.* RNA buffers the phase separation behavior of prion-like RNA binding proteins. *Science* **360**, 918–921 (2018).
19. Qamar, S. *et al.* FUS Phase Separation Is Modulated by a Molecular Chaperone and Methylation of Arginine Cation-π Interactions. *Cell* **173**, 720-734.e15 (2018).
20. Dormann, D. *et al.* ALS-associated fused in sarcoma (FUS) mutations disrupt Transportin-mediated nuclear import. *The EMBO Journal* **29**, 2841–2857 (2010).
21. Dormann, D. & Haass, C. Fused in sarcoma (FUS): An oncogene goes awry in neurodegeneration. *Molecular and Cellular Neuroscience* **56**, 475–486 (2013).
22. Tong, X. *et al.* Liquid–liquid phase separation in tumor biology. *Signal Transduction and Targeted Therapy* **7**, 221 (2022).
23. Boija, A., Klein, I. A. & Young, R. A. Biomolecular Condensates and Cancer. *Cancer Cell* **39**, 174–192 (2021).
24. Ji, Y., Li, F. & Qiao, Y. Modulating liquid–liquid phase separation of FUS: mechanisms and strategies. *J. Mater. Chem. B* **10**, 8616–8628 (2022).
25. Krainer, G. *et al.* Reentrant liquid condensate phase of proteins is stabilized by hydrophobic and non-ionic interactions. *Nature Communications* **12**, 1085 (2021).
26. Kozlov, A. G. *et al.* How Glutamate Promotes Liquid-liquid Phase Separation and DNA Binding Cooperativity of E. coli SSB Protein. *Journal of Molecular Biology* **434**, 167562 (2022).
27. Wang, X., Schwartz, J. C. & Cech, T. R. Nucleic acid-binding specificity of human FUS protein. *Nucleic Acids Research* **43**, 7535–7543 (2015).
28. Mullard, A. & others. Biomolecular condensates pique drug discovery curiosity. *Nat. Rev. Drug Discov* **18**, 324–326 (2019).
29. Mitrea, D. M., Mittasch, M., Gomes, B. F., Klein, I. A. & Murcko, M. A. Modulating biomolecular condensates: a novel approach to drug discovery. *Nature Reviews Drug Discovery* **21**, 841–862 (2022).
30. Ambadipudi, S., Reddy, J. G., Biernat, J., Mandelkow, E. & Zweckstetter, M. Residue-specific identification of phase separation hot spots of Alzheimer's-related protein tau. *Chem. Sci.* **10**, 6503–6507 (2019).
31. Yamazaki, T. *et al.* Functional Domains of NEAT1 Architectural lncRNA Induce Paraspeckle Assembly through Phase Separation. *Molecular Cell* **70**, 1038-1053.e7 (2018).
32. Strom, A. R. *et al.* Phase separation drives heterochromatin domain formation. *Nature* **547**, 241–245 (2017).
33. Lu, H. *et al.* Phase-separation mechanism for C-terminal hyperphosphorylation of RNA polymerase II. *Nature* **558**, 318–323 (2018).
34. Mastrocola, A. S., Kim, S. H., Trinh, A. T., Rodenkirch, L. A. & Tibbetts, R. S. The RNA-binding Protein Fused in Sarcoma (FUS) Functions Downstream of Poly(ADP-ribose) Polymerase (PARP) in Response to DNA Damage *. *Journal of Biological Chemistry* **288**, 24731–24741 (2013).
35. Arter, W. E. *et al.* Rapid Generation of Protein Condensate Phase Diagrams Using Combinatorial Droplet Microfluidics. *bioRxiv* 2020.06.04.132308 (2020) doi:10.1101/2020.06.04.132308.
36. McCarty, J., Delaney, K. T., Danielsen, S. P. O., Fredrickson, G. H. & Shea, J.-E. Complete Phase Diagram for Liquid–Liquid Phase Separation of Intrinsically Disordered Proteins. *J. Phys. Chem. Lett.* **10**, 1644–1652 (2019).
37. Villois, A. *et al.* Droplet Microfluidics for the Label-Free Extraction of Complete Phase Diagrams and Kinetics of Liquid–Liquid Phase Separation in Finite Volumes. *Small* **n/a**, 2202606 (2022).
38. Eftink, M. R. Fluorescence Quenching: Theory and Applications. in *Topics in Fluorescence Spectroscopy: Principles* (ed. Lakowicz, J. R.) 53–126 (Springer US, 2002). doi:10.1007/0-306-47058-6_2.
39. Qian, D. *et al.* Tie-lines reveal interactions driving heteromolecular condensate formation. *bioRxiv* 2022.02.22.481401 (2022) doi:10.1101/2022.02.22.481401.
40. Welsh, T. J. *et al.* Surface Electrostatics Govern the Emulsion Stability of Biomolecular Condensates. *Nano Lett* **22**, 612–621 (2022).
41. Dignon, G. L., Best, R. B. & Mittal, J. Biomolecular Phase Separation: From Molecular Driving Forces to Macroscopic Properties. *Annu Rev Phys Chem* **71**, 53–75 (2020).
42. Ausserwöger, H. *et al.* Surface interaction patches link non-specific binding and phase separation of antibodies. *bioRxiv* 2022.03.07.483238 (2022) doi:10.1101/2022.03.07.483238.
43. Li, L. *et al.* Phase Behavior and Salt Partitioning in Polyelectrolyte Complex Coacervates. *Macromolecules* **51**, 2988–2995 (2018).

44. Friedowitz, S. *et al.* Looping-in complexation and ion partitioning in nonstoichiometric polyelectrolyte mixtures. *Science Advances* **7**, eabg8654.
45. Suhling, K. *et al.* Fluorescence lifetime imaging (FLIM): Basic concepts and some recent developments. *Medical Photonics* **27**, 3–40 (2015).
46. Suhling, K. *et al.* Imaging the Environment of Green Fluorescent Protein. *Biophysical Journal* **83**, 3589–3595 (2002).
47. CACACE, M. G., LANDAU, E. M. & RAMSDEN, J. J. The Hofmeister series: salt and solvent effects on interfacial phenomena. *Quarterly Reviews of Biophysics* **30**, 241–277 (1997).
48. Kroschwald, S., Maharana, S. & Alberti, S. Hexanediol: a chemical probe to investigate the material properties of membrane-less compartments. *Matters* (2017) doi:10.19185/matters.201702000010.
49. Düster, R., Kaltheuner, I. H., Schmitz, M. & Geyer, M. 1,6-Hexanediol, commonly used to dissolve liquid–liquid phase separated condensates, directly impairs kinase and phosphatase activities. *Journal of Biological Chemistry* **296**, (2021).
50. Arosio, P. *et al.* Microfluidic Diffusion Analysis of the Sizes and Interactions of Proteins under Native Solution Conditions. *ACS Nano* **10**, 333–341 (2016).
51. Chen, C., Ding, X., Akram, N., Xue, S. & Luo, S.-Z. Fused in Sarcoma: Properties, Self-Assembly and Correlation with Neurodegenerative Diseases. *Molecules* **24**, (2019).
52. Liu, X. *et al.* The RRM domain of human fused in sarcoma protein reveals a non-canonical nucleic acid binding site. *Biochimica et Biophysica Acta (BBA) - Molecular Basis of Disease* **1832**, 375–385 (2013).
53. Krainer, G. *et al.* Direct digital sensing of protein biomarkers in solution. *bioRxiv* 2020.05.24.113498 (2022) doi:10.1101/2020.05.24.113498.
54. Kim, S., Ma, L., Unruh, J., McKinney, S. & Yu, C. R. Intracellular chloride concentration of the mouse vomeronasal neuron. *BMC Neuroscience* **16**, 90 (2015).
55. Gururaja Rao, S., Patel, N. J. & Singh, H. Intracellular chloride channels: novel biomarkers in diseases. *Frontiers in physiology* **11**, 96 (2020).
56. Peretti, M. *et al.* Chloride channels in cancer: Focus on chloride intracellular channel 1 and 4 (CLIC1 AND CLIC4) proteins in tumor development and as novel therapeutic targets. *Biochimica et Biophysica Acta (BBA) - Biomembranes* **1848**, 2523–2531 (2015).

Conflicts of interest

The authors declare no conflicts of interest.

Acknowledgements

The research leading to these results has received funding from Global Research Technologies, Novo Nordisk A/S (H.A., T.P.J.K.), the European Research Council under the European Union's Horizon 2020 Framework Programme through the Marie Sklodowska-Curie grant MicroSPARK (agreement no. 841466; G.K.), the Herchel Smith Funds (G.K.), the Alzheimer Association Zenith Award (P.S.G.-H.) and the Wolfson College Junior Research Fellowship (G.K.). T.J.W. thanks the Harding Distinguished Postgraduate Scholar Programme.

Author contributions

H.A., D.Q., G.K., T.J.W., and T.P.J.K. designed and conceptualized the study. H.A. performed experiments. G.K., T.J.W., T.S., T.M.F., S.Q. and P.S.G.-H. provided materials and methods. H.A. and D.Q. analysed the data. H.A., D.Q., G.K., T.J.W., J.N.A., M.K., R.V.P. and T.P.J.K. interpreted data. H.A. and G.K. wrote the original draft of the paper. All authors discussed the results, commented on the manuscript, and contributed to the final manuscript.

Correspondence

Correspondence and requests for materials should be addressed to Tuomas P. J. Knowles (tpjk2@cam.ac.uk).

Data availability

The raw data and analysis code underlying this study will be made available upon reasonable request.